RESEARCH ARTICLE | SEPTEMBER 05 2023

Experimental and theoretical investigations of the radiation-induced conductivity in spacecraft polymers at extremely low temperatures ⊘

Andrey Tyutnev ⓘ ; Vladimir Saenko ✉ ⓘ ; Ilshat Mullakhmetov ⓘ ; Evgenii Pozhidaev ⓘ

Check for updates

🌐 View Online 📄 Export Citation CrossMark

Articles You May Be Interested In

A functional integral formalism for quantum spin systems

J. Math. Phys. (July 2008)

08 September 2023 05:38:44

Experimental and theoretical investigations of the radiation-induced conductivity in spacecraft polymers at extremely low temperatures

Andrey Tyutnev,[a)] (iD) Vladimir Saenko,[b)] (iD) Ilshat Mullakhmetov, (iD) and Evgenii Pozhidaev (iD)

AFFILIATIONS

National Research University Higher School of Economics, 20 Miasnitskaya Ulitsa, Moscow 101000, Russia

[a)]Electronic mail: aptyutnev@yandex.ru
[b)]Author to whom correspondence should be addressed: saenko19@gmail.com

ABSTRACT

Radiation-induced conductivity (RIC) of polyethyleneterepfthalate and polypiromellitimide has been studied experimentally and numerically in a broad time range from some microseconds to seconds at 103 K. It has been established that the charge carrier transport is dispersive with a low value of the dispersion parameter α (0.08–0.12). We have suggested a direct method of determination of the frequency factor of the Rose–Fowler–Vaisberg (RFV) model, which has been parameterized using computer simulations by the trial-and-error method. The main concern is a critical analysis of the existing theories of geminate recombination. It has been shown that the traditional RFV model is well suited to describe the RIC in studied polymers even at 103 K if due corrections to the notion of a *free* charge carrier and a non-Langevin bimolecular recombination have been made. The problem of a space charge field due to beam electrons stopped in a polymer sample, which is especially important at low temperatures, has been accounted for but not fully explained.

Published under an exclusive license by AIP Publishing. https://doi.org/10.1063/5.0158855

I. INTRODUCTION

Our previous studies of the radiation-induced conductivity (RIC) in spacecraft polymers were restricted to room and higher temperatures.[1] Since that time, we have greatly improved experimental methodology combining pulsed and long-time irradiations, which allowed us to develop further the mainstream theoretical tool [the semiempirical Rose–Fowler–Vaisberg (RFV) model].[2] Using it, we were able to treat the RIC phenomenon almost on a quantitative basis. Recently, we extended RIC investigations to extremely low temperatures (up to 79 K) using polystyrene (PS) as a prototype polymer featuring an exponential trap distribution.[3] Spacecraft polymers as a rule have a much more complicated trap structure[2] and require a more detailed consideration. In this paper, we investigated two most popular spacecraft polymers polyethyleneterepfthalate (PET) and polypiromellitimide (PI) finding wide application as thermal blankets on spacecraft outer surfaces. These polymers are expected to withstand as low temperatures as minus 150 °C (123 K). So, we selected for our studies a slightly lower temperature 103 K.

In our latest work,[3] we managed to describe the RIC of PS at 79 K using the RFV model rather adequately but some mute points have been encountered concerning charge carrier recombination, the free ion yield and the possible role of beam electrons being stopped in a test sample, an effect which is expected to become especially important at these low temperatures. It is the purpose of the present paper to investigate commercial films of PET and PI, to prove, if only on a limited scale, the RFV theory at low temperatures and to give a critical consideration of the two most advanced theories of the geminate conductivity in disordered solid media, developed by Russian scientists first for frozen organic glasses[4,5] and later for disordered solids.[6,7] It has been shown that *at early times* $t \leq t_{inv}$ (for details, see Sec. IV) *geminate electrons behave like free charges.* This conclusion justifies parameterization of the RFV model for PS[3] based on experiments conducted at these early times at 79 K. An observed time of a current maximum t_m (see Sec. VI) was found to be around 35 s but it was measured for only one dose rate 13 Gy/s. Now, we would like to extend these measurements to a range of dose rates in all polymers and investigate the origin of the latter time in detail.
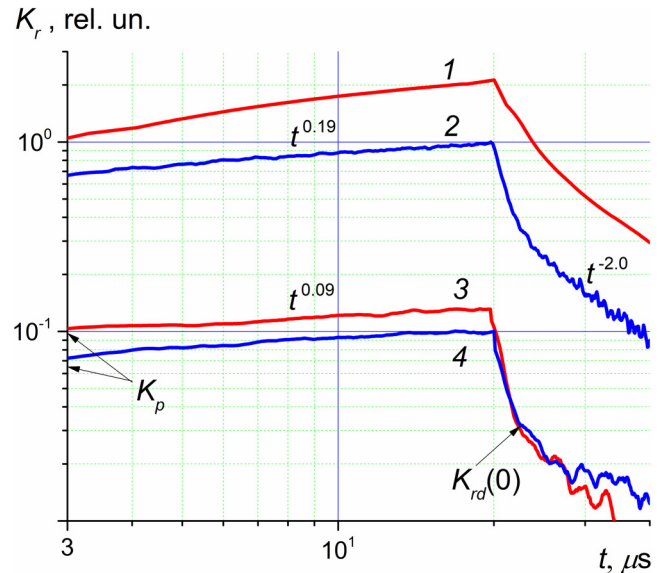
II. EXPERIMENTAL

A. Methodology

Investigated polymers include Russian-made PET films $15\,\mu m$ thick (PET-1, Vladimir Chemical Works, RF), $5\,\mu m$ thick (PET-2, Institute of Space and Aviation Materials, Pereyaslav-Zalesskii, Yaroslav Region, RF) taken from a thermal blanket of an operational spacecraft, and PI (Kapton, Du Pont, Wilmington, DE, USA) films $25\,\mu m$ thick. Also, as a reference polymer, we used PS (Styroflex, Norddeutsche Seekabelwerke AG, Nordenham, FRG) films $20\,\mu m$ thick studied earlier.[2,3] Specimens (40 mm in diameter) were supplied with evaporated 50 nm Al electrodes 32 mm in diameter. We used only *fresh* samples for each long-time irradiation run. Note that a low temperature long-time experiment takes a whole day and, thus, proves to be not only material but time expensive as well. Experiments have been conducted at 103 K and most data refer to an electric field 4×10^7 V/m if not stated otherwise.

As usual, we used an ELA-50 electron gun (Orion, Moscow, RF) as an irradiation source modified to accommodate low temperature measurements. Monoenergetic 50-keV electrons fall normally upon a sample holder. Pulse fronts were reduced to $2.5\,\mu s$ and dose rates were constant to within 5% during continuous irradiation. A shutter with an opening time of 0.08 s is used to set the beam current beforehand and manually control it during a continuous irradiation. Compared to our previous studies of RIC in polymers conducted at room temperature,[1,2,8–10] the measuring cell has been radically modified to accommodate RIC measurements at liquid nitrogen temperature.[3] As a result, a beam current of 1 nA measured by the shutter would correspond to a dose rate of 2.5 Gy/s in both polymers compared with 1.9 Gy/s reported earlier.[8] Irradiation and measuring techniques were treated in detail in Ref. 8 and will be considered later in Sec. V in relation with electron charging effects accompanying RIC measurements.

An experimentally measured quantity is the RIC current density j_r. The raw pulse data were processed to separate the delayed component j_{rd} from the total signal: $j_{rd} = j_r - j_p$ where j_p is the RIC prompt component.[1] In the case of a small-signal irradiation, we introduce the normalized quantities: the conductivity $\gamma_r = j_r/F_0$ and the conductivity reduced per unit dose rate $K_r = \gamma_r/R_0$ separating delayed and prompt components (low indices for r being rd and p, respectively).

B. Experimental results

RIC results obtained for a pulse length of $20\,\mu s$ are given in Fig. 1. Pulse fronts (about $3\,\mu s$) complicate appreciably studying the kinetics of a current build-up and decay immediately after the pulse end. We see that K_r measured at low temperatures is appreciably smaller (by at least a factor of 8) than at room temperature and is close to their prompt conductivity. In PS,[3] this effect was appreciably stronger. Evaluation of the reduced prompt conductivity K_p requires measurements at the shortest times possible to lower the contribution of a delayed component which was effectively achieved in PET, but not in Kapton (Fig. 1). RF noise and RC distortion limit signal registration to a time interval from 3 to $40\,\mu s$ only (as shown in the figure).

FIG. 1. Experimental RIC current transients registered in PET-1 (*1*, *3*, red) and Kapton (*2*, *4*, blue) at 103 (lower curves, *3*, *4*) and 290 K (upper curves, *1*, *2*) all taken in a small-irradiation regime at a dose rate of 5×10^5 Gy/s (pulse dose 10 Gy). RC is equal to 0.1 (103 K) and $1\,\mu s$ (295 K). Rel. unit is equal to $1.6 \times 10^{-14}\,\Omega^{-1}\,m^{-1}\,Gy^{-1}$ s. $K_{rd}(0)$ means K_{rd} measured at a pulse end.

Previous measurements of K_p at room temperature at a field of 10^7 V/m using triangular $3\,\mu s$ pulses gave the following results: $K_p = 1.6$ (PET), 1.0 (Kapton), and 3.5 (PS) all in units $10^{-15}\,\Omega^{-1}\,m^{-1}\,Gy^{-1}$ s, accurate to ±20%. These unpublished results were obtained in Ref. 2 and were used in the present paper as initial values to assess the frequency factor ν_0 of the RFV model (see Sec. III). Table I presents the results of pulsed RIC measurements in our polymers at a low temperature.

Unlike Ref. 3, in the present work, short pulses of radiation (10–20 μs long) have become available but we failed to measure current–voltage characteristics (VAC) for prompt and delayed components of RIC in PET-1 and Kapton due to small signals and an excessive RF noise. But we managed to ascertain that the VAC for the prompt conductivity in PS was still linear in going from 2 to 4×10^7 V/m contrary to Fig. 4 in Ref. 3. We ascribe this discrepancy to the fact that in Ref. 3, we had to use 1 ms pulses and the

TABLE I. Experimentally determined values of K_r taken at indicated times in a small-signal regime (all in units of $10^{-15}\,\Omega^{-1}\,m^{-1}\,Gy^{-1}$ s) at 103 K. K_p values are those indicated earlier.

Polymer	Parameter		
	K_p	K_r at $20\,\mu s$	K_r at 1 ms
PET-1	1.6	2.1	3.2
PET-2	...	...	...
Kapton	1.0	1.6	2.4

contribution of a delayed component in the early part of the pulse was not sufficiently small.

Now, we would like to consider current transients taken under continuous irradiation at 103 K (Fig. 2). They resemble very much those predicted by the RFV model and observed in PS at room and liquid nitrogen temperatures.[2,3] Again, the current rises as $j_r \propto t^\alpha$ until $t \approx 0.1 \times t_m$ (at t_m it reaches the maximum j_m) and later it decays as a power function $j_r \propto t^{-\beta}$ with exponent β being remarkably less than unity (0.1–0.25). It is tempting to identify t_m with the theoretical t_{inv} introduced in Ref. 6 but our analysis in Secs. IV and VI proves that this question still remains unresolved.

The peculiar RIC rising with an accumulated dose observed in Kapton[9] (see curve 2 in Fig. 2) vanishes and is replaced by a standard response given by the multiple trapping (MT) formalism.[1,2]

It is important that j_r rises as t^α (Fig. 2) with dispersion parameter α being around 0.08–0.12, this fact being in line with a low experimental temperature. In fact, the general expression for α can be written as follows:[3]

$$\alpha(T) = \alpha(T_0) \times (T/T_0). \tag{1}$$

Here, T is a current temperature and T_0 is a reference temperature (usually, room temperature). In PET and Kapton, one should use α measured during the first $20\,\mu s$ of pulsed irradiations at room temperature (0.3–0.5 as in Ref. 2) to obtain the above-cited data.

As already stated in Sec. I, we add information concerning the variation of t_m as a function of the dose rate for all three polymers. Figure 3 shows that this behavior is rather chaotic but some facts have been firmly established. First, t_m is not a constant in all tested polymers (in PS, it has been demonstrated just in the present
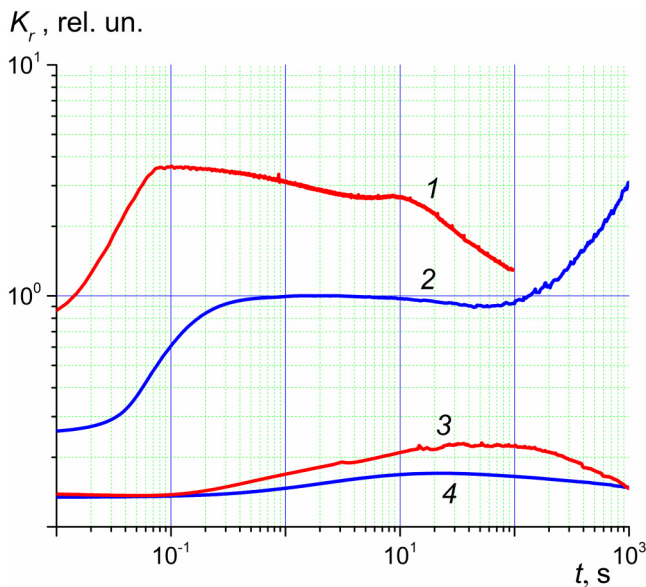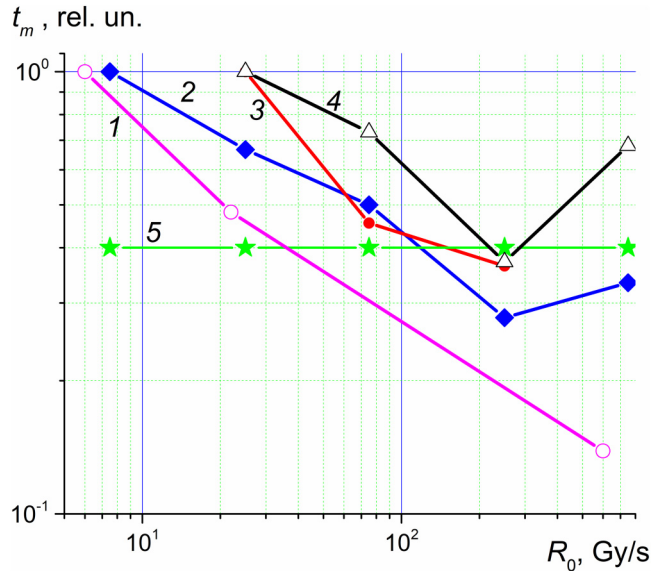

FIG. 3. Dependence of t_m for PET-2 (1, magenta), Kapton (2, blue), PS (3, red), PET-1 (4, black), Arkhipov theoretical model[6] (5, green) on dose rate. Note: every data point was taken on a fresh sample only expending a whole working shift for this purpose.

work). Second, there is a clear tendency of it diminishing with a rising dose rate. Absolute values of t_m calculated according to the model of Arkhipov et al.[6,7] (Table II) and their correlation with experimental data are considered in Sec. IV.

Parameter K_{rm} allows, if only approximately, estimating the maximum conductivity in a polymer under continuous irradiation:

$$\gamma_{rm} = K_{rm}R_0. \tag{2}$$

For rough engineering usage in the appraisal of electron charging of satellite thermal blankets in the dark, Eq. (2) is very useful, especially if it is taken to mean a universal value for both polymers of $10^{-14}\,\Omega^{-1}\,m^{-1}\,Gy^{-1}$ s. Figure 4 presents γ_m as a function of R_0 for all polymers including PS. Like in Fig. 3, scatter of data points is obvious with an exception of curves 1 and 2 for

FIG. 2. Current transients for long-time irradiations in PET-1 (1 and 3, red), Kapton (2 and 4, blue) measured at 250 Gy/s. Temperature 103 (lower curves) and 290 K (upper curves). Rel. unit is equal to $4.4 \times 10^{-14}\,\Omega^{-1}\,m^{-1}\,Gy^{-1}$ s.

TABLE II. RFV parameters for tested polymers at 4×10^7 V/m and 103 K. Data for t_{inv} refer to values of r_0 given in brackets (for details, see Sec. IV).

| Parameter | Polymer | | |
	PET-1,2	Kapton	PS[3]
α	0.11	0.11	0.09
$\mu_0 \times 10^5$, m²/V s	1.0	1.0	1.0
$\tau_0 \times 10^{11}$, s	0.38	0.24	1.75
$\nu_0 \times 10^{-5}$, s⁻¹	4.0	10.0	0.04
t_{inv}, s	0.005 (6 nm)	0.6 (6 nm)	9.2 μs (6 nm)
	3.2 (7 nm)	40.3 (7 nm)	1.6 ms (7 nm)
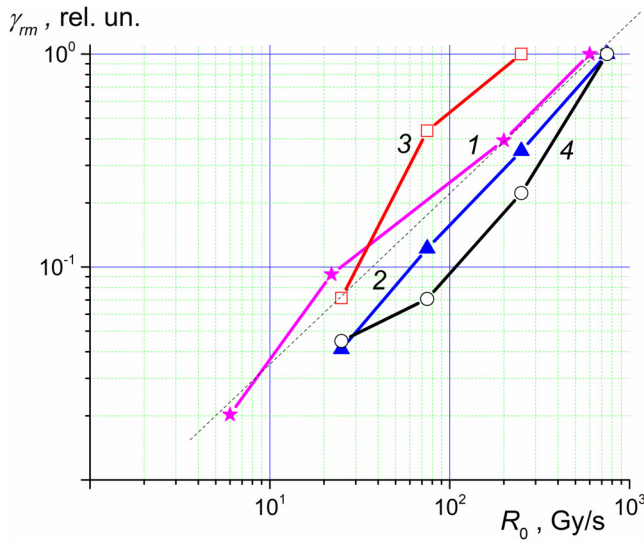
FIG. 4. Rad-ampere characteristics at maximum RIC registered in PET-2 (1, magenta), Kapton (2, blue), PS (3, red), and PET-1 (4, black). Dose rate 200 (1) and 250 Gy/s (2 and 3), temperature 103 K. Dashed straight line approximates curve 1. See note on Fig. 3.

PET-2 and Kapton, respectively. In PET-2 samples, the rad-ampere characteristic took the form differing from Eq. (2) but which is expected for the RFV model,[1]

$$\gamma_{rm} = A_{rm}R_0^\Delta, \tag{3}$$

where A_{rm} is a constant and $\Delta = (1 + \alpha)^{-1}$.[1] The measured value of Δ is 0.84 (curve 1 in Fig. 4), which is rather close to its predicted value for $\alpha \approx 0.12$ (0.89) as this figure demonstrates. Possible reason for normal behavior of RIC data in PET-2 will be given in Sec. V linking it with an electron charging phenomenon.

The current maximum is nearly proportional to the dose rate $j_m \propto R_0$ as Fig. 4 shows. At room temperature, both polymers show exactly this type of behavior ($j_m \propto R_0^\Delta$ with $\Delta \approx 1$) due to a complex trap structure (two exponential distributions joined at energy E_S[2]). But at 103 K, only shallow traps are operative while an effect of deep traps is shifted beyond observation times.[10] The most spectacular result of low temperature irradiations is a disappearance of peculiar transient shapes shown earlier in Fig. 2 for Kapton.

III. ESTIMATION OF RFV PARAMETERS

The dose rate g_0 (a theoretical input parameter) is proportional to R_0 (an experimental output parameter) with $\eta_0 = g_0/R_0$ depending on the details of a charge generation process. Generally, η_0 may be calculated from the following formula:[3]

$$g_0(m^{-3}s^{-1}) = 6.24 \times 10^{19}\rho G R_0 \text{ (Gy/s)}, \tag{4}$$

where ρ is density (g/cm³) and G is the radiation yield per 100 eV of the absorbed energy of charge carriers taking part in the

conduction process. In the RFV model $G \equiv G_{fi}$, the radiation yield of free charge carriers.[11–13] At 79–103 K, quantity G should mean G_i, the initial radiation yield of geminate electrons which is equal to 3.0 (the probability of trapping is unity[7]). Taking polymer density as 1.4 g/cm³ (PI and PET), we finally obtain

$$\eta_0 = 2.6 \times 10^{20} \text{ m}^{-3}\text{Gy}^{-1}. \tag{5}$$

For a typical dose rate of 100 Gy/s, we have $g_0 = 2.6 \times 10^{22} \text{ m}^{-3} \text{ s}^{-1}$.

Now, we would like to parameterize the RFV model for test polymers similar to what has been done for PS in Ref. 3. We continue to use the RFV model as the most useful semiempirical tool to describe charge transport in disordered solids on a microscopic level. The basic equations of this model are well known,[1–3]

$$\begin{cases} \dfrac{dN(t)}{dt} = g_0 - k_{rec}N_0(t)N(t), \\ \dfrac{\partial\rho(E,t)}{\partial t} = k_cN_0(t)\left[\dfrac{M_0}{E_1}\exp\left(-\dfrac{E}{E_1}\right) - \rho(E,t)\right] - v_0\exp\left(-\dfrac{E}{kT}\right)\rho(E,t), \\ N(t) = N_0(t) + \int\limits_0^\infty \rho(E,t)dE, \end{cases} \tag{6}$$

where both $N_0(t)$ and $\rho(E,t)$ are zero at $t = 0$. By definition, the RIC is $\gamma_r(t) = e\mu_0N_0(t)$. Thus, this system refers to a unipolar conduction with only one sign carriers being mobile (in our case, electrons). Holes are immobile and act as recombination centers.

Here, $N(t)$ is the total concentration of radiation-produced electrons (due to charge neutrality, equal to that of holes). $N_0(t)$ is an electron concentration in extended states (in the conduction band) with the microscopic mobility μ_0, g_0 is the generation rate of free electrons (assumed time and space independent during irradiation), k_{rec} is the recombination coefficient, k_c is the trapping rate constant, M_0 is the total concentration of traps distributed exponentially in energy E (taken positive) with the distribution parameter E_1, $\rho(E,t)$ is the time dependent density distribution of trapped electrons, v_0 is the frequency factor, T is the temperature, k is Boltzmann's constant, and e is the elementary electric charge. Also, $\tau_0 = (k_cM_0)^{-1}$ is the lifetime of mobile electrons before trapping. The dispersion parameter $\alpha = kT/E_1$. The second and third equations in system (6) are generic for a quasi-band description of the charge carrier transport in a disordered dielectric and are generally known as the MT formalism. The first equation (the continuity relation) in the present form describes a typical one-dimensional RIC problem in a polymer featuring the Langevin bulk recombination as in our polymers at room temperature. At 77 K, the recombination may no longer be such a process but we continue to use a Langevin-type recombination coefficient (see Sec. VI).

The main model parameters are as follows: dispersion parameter α, electron microscopic mobility μ_0 and its lifetime τ_0 (the last two parameters enter basic formulas as their product only), and the frequency factor v_0. The first and the last of them may be found directly from the experiment. In accord with Ref. 3, we assume that a theoretical $K_p' = \eta_0\mu_0\tau_0 e$ coincides with an experimental K_p. This assumption allows finding $\mu_0\tau_0$ in one step and v_0 by means of an

iteration procedure using MathCad calculations to be finalized by RFV simulations.

For direct assessment of the frequency factor ν_0, we employed the procedure described in Ref. 14 analyzing the form of a decay curve just after the pulse end. If it looks like a straight line on a $\lg j - \lg t$ plot (which seems to be the case for PET-1 at 103 K as Fig. 1 shows), then a simple relationship holds $\nu_0 \times t_p \approx 4.0$. If it is concave, it means only that $\nu_0 \geq t_p^{-1}$. In the case of a convex curve, the approximate assessment of the frequency factor is also possible: $\nu_0 \approx t_k^{-1}$, where t_k is the time of the kink. This technique was effectively used in our previous studies.[1]

We performed MathCad calculations based on the analytical treatment developed by Nikitenko et al.[15] By the way, numerical simulations using the RFV model fully confirmed MathCad calculations. Also, we found it useful to measure the RIC at the end of the $20\,\mu s$ pulse and at $100\,\mu s$ after its end. Using these data for MathCad simulations for known α allowed us to assess ν_0 as described in Ref. 9. Of course, we used also an indirect approach of assessing ν_0 by fitting K_r at certain times (Table I) using values of the product $\mu_0\tau_0$ determined from K_p. The best fitting RFV parameters are given in Table II which contains also calculated values of t_{inv} [see Eq. (7) in Sec. IV].

Now that RFV parameters have been determined, we may proceed with numerical calculations aiming to compare theoretical predictions with experimental results for both pulsed and continuous irradiations (Fig. 5) to be used in Sec. VI.

We see that the RFV model is able to reproduce experimental RIC data from 10^{-8} s to almost t_m. The predicted value of Δ is 0.89 as already mentioned in Sec. II B [Eq. (3)]. After t_m, experimental curve decreases rather slower than a theoretical one. It is interesting that predicted and experimental maximum times almost coincide at 75 Gy/s
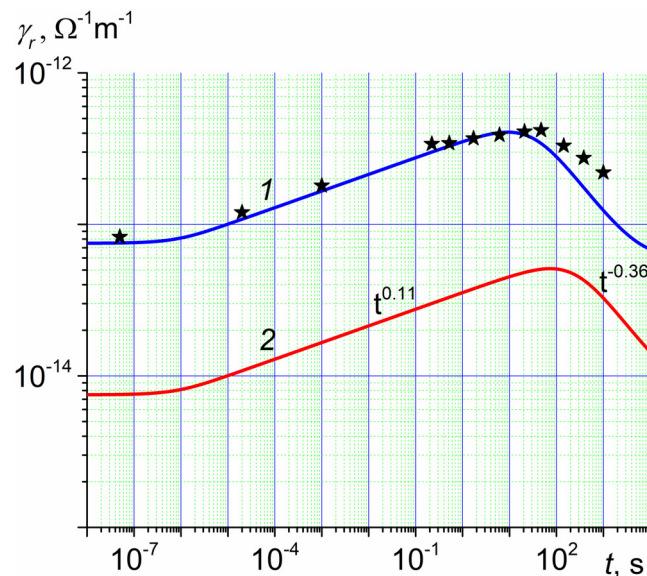

FIG. 5. Comparison of calculated RFV curves with experimental data points (curve *1*) for Kapton at dose rates 75 (curve *1*, blue) and 7.5 Gy/s (curve *2*, red). Data points are marked as stars.

(curve *1*). Of course, at other values of a dose rate, this agreement will become poorer (see Fig. 3) but such a fact is really remarkable.

IV. INTERPRETATION OF RESULTS

Once MT parameters of a polymer at a low temperature have been determined, it becomes possible to test predictions of competing models in explaining the origin of a current limitation in the long-time, low-temperature irradiations observed at t_m. The RFV model associates it with a bimolecular diffusion-controlled recombination according to the Langevin mechanism. It predicts that the product $t_m\gamma_{rm}$ does not change with a dose rate. This fundamental property breaks down on a quantitative level, but not qualitatively (increasing R_0 tends to diminish t_m in all polymers including PS as Fig. 3 demonstrates). It seems that some other mechanism of bimolecular recombination comes into play in these conditions.

This situation is better understood using the theoretical results of Arkhipov et al.[7] relating to the geminate conductivity in a disordered solid irradiated at low temperature (around 77 K) in the presence of an electric field (which exactly match our experimental conditions). A model polymer is assumed to be a one-carrier (specifically, electron) conductor to reconcile the radiation chemistry language with a multiple trapping formalism used in the radiation physics of disordered solids.[1,2]

The analysis considers the dispersive Smoluchowski equation in a drift-only approximation (diffusion neglected).[7] In this case, an electron drifts only along field lines and the famous drift-diffusion equations[13] are no longer valid. The main results refer to the current density $j_\delta(t)$ and the surviving probability $\Omega(t)$ of geminate electrons following a δ-pulse generation of non-interacting (but already stabilized) geminate pairs, which are uniformly distributed and randomly oriented in space, all with the same separation distance between sibling charges in a pair r_0.

From an experimental point of view, the most important quantity is a step-function solution $j(t)$, which is obtained by convoluting $j_\delta(t)$ in time. Evidently, $j(t)$ corresponds to a current transient observed during a long-time (continuous) irradiation. The field criterion is $\psi_0 = F_0/F_c$, where $F_c = e/4\pi\varepsilon\varepsilon_0 r_0^2$ is the Coulomb field at distance r_0—an initial electron-hole separation in a geminate pair, ε is the relative dielectric constant, and ε_0 is the dielectric constant. For $\psi_0 \leq 1$, fields are considered to be small while for $\psi_0 > 1.1$ they are strong.

We see that F_c depends critically on r_0. The most popular value of r_0 in polymers is 6 nm as in polyvinylcarbazole and PS[16–18] which means that for them, $\psi_0 = 3.2 > 1.1$ and our field 4×10^7 V/m is a strong one. According to theory, the survival probability $\Omega(t \to \infty) = \Omega_\infty = 1 - \psi_0^{-1}$ and is equal to 0.69 in our case. It is predicted that $j_\delta(t) \propto \Omega(t) \times t^{-1+\alpha}$ where transition of the term $\Omega(t)$ from unity to Ω_∞ terminates in about 30 t_{inv}, which may be taken as the geminate lifetime t_g. The time t_{inv} (the so-called inversion time) is given by the following expression:

$$t_{inv} = \nu_0^{-1} \left[\frac{4\pi\varepsilon\varepsilon_0}{3e\mu_0\tau_0} r_0^3 \right]^{1/\alpha}. \tag{7}$$

Of course, a transient current $j(t)$ can be described by an analogous formula $j(t) \propto \Omega(t) \times t^{1-\alpha}$. This analysis shows that the

above theory duplicates RFV result with a correction factor $\Omega(t)$ decreasing from unity to 0.69 during pair lifetime t_g.

Now, we should address a case of low r_0. To make the field 4×10^7 V/m small, we have to use $r_0 \leq 3$ nm but even a slightly larger value $r_0 = 3.5$ nm in PET was cited in the literature only once.[19]

In this case, the above picture dramatically changes.[6,7] First, $\Omega(t)$ decreases asymptotically as $\Omega \propto t^{-\alpha}$ leading to $\Omega_\infty = 0$. Second, $j_\delta(t)$ changes sign at t_{inv} (this is the reason for its name), peaking at 2.1 t_{inv} (about 0.01 of its initial value by module) and then falling asymptotically (in absolute value also) as $t^{-1-\alpha}$ approaching zero from below. Naturally, a time integral of the current $j_\delta(t)$ is zero. Estimated inversion times in our polymers are presented in Table II. By convoluting $j_\delta(t)$, one obtains a step-function current $j(t)$ which rises initially as $j \propto t^\alpha$, reaches a maximum j_m at $\hat{t}_m$, and then falls asymptotically as $j \propto t^{-\alpha}$, the curve being symmetrical about $\hat{t}_m$. As expected, j_m is proportional to the light intensity with $\hat{t}_m$ *being independent of it*. An important relation $t_{inv} \approx \hat{t}_m$ connects a δ-pulse with the step-function excitation mode. It is tempting to identify $\hat{t}_m$ with an experimental t_m (Fig. 2). But one serious objection is that $\hat{t}_m$ would be about some nanoseconds for $r_0 = 3$ nm, which contradicts to experimental values of t_m (10–100 s). Besides, the predicted current would fall as $j \propto t^{-\alpha}$ instead of rising as $j \propto t^\alpha$ (curves *3* and *4* in Fig. 2). We conclude that this assumption is not acceptable in our case. So, the best theoretical model to describe RIC in PET, Kapton, and PS is the RFV model with yet uncertain recombination term.

It should be reminded that Arkhipov *et al.* considered generation of *non-interacting (isolated)* geminate pairs and obtained that the current density $j \propto \Omega(t) \times t^{1-\alpha}$ would grow to infinity at long times. But we have to take into account the fact that continued irradiation creates a random lattice of immobile holes with ever increasing concentration. Drift lines of free electrons start inevitably hitting capture spheres centered on these holes. An encounter of a free electron with a capture sphere would result in an electron recombination only if its radius is small (about 3 nm or even less). Otherwise, an electron would drift along with only a slight perturbation of its trajectory. Probably, it is the reason for the appearance of the non-Langevin recombination.[20,21]

In 1994,[22] we have already developed a similar approach explaining a controversial room-temperature RIC behavior in polymers at a strong electric field of 5×10^7 V/m. Experimental data covered a broad range of irradiation times (from 1 ms to 10 s covering every decade including a $4 \mu s$ pulse length). It has been shown that in polymers featuring geminate conductivity and $r_0 \approx 6$ nm (polytetrafluoroethylene, polyethylene, polypropylene, polyvinyl fluoride) the free ion yield is close to G_i and is almost field independent. Also, full charge collection has been observed[23] (recently, we confirmed this result in Ref. 2) while the non-Langevin recombination has been associated with a substantially reduced recombination rate compared with a drift-controlled Langevin mechanism. In the opposite case ($r_0 \leq 3$ nm), the RIC gets low approaching its prompt conductivity as in polymethylmethacrylate and polyvinylchloride. Evidently, there is a need of conducting computer simulations of a geminate conductivity in disordered solids similar to what has been done in Ref. 24 for an ideal trap-free dielectric.

We see that both the RFV model and the general theory of the geminate conductivity apply equally well for interpretation of the obtained RIC results but only for irradiation times less than t_m, which are suspiciously close to the Maxwell relaxation time for γ_{rm}. Note that both abovementioned theories do not consider the presence of the space charge field and its influence on the traditional results. So, we need to consider the role of the electron charging of a test sample more carefully.

V. EFFECTS OF ELECTRON CHARGING

RIC measurements using electron guns are accompanied by two physical phenomena, which essentially complicate an interpretation of experimental results, namely, the depth distribution of a dose rate and an electron deposition rate in a polymer sample. The problem of a dose rate non-uniformity has been successfully solved by proper averaging the universal dose depth profile of electrons with 20–100 keV energy.[9] The second phenomenon was found insignificant at room temperature RIC studies due to a small magnitude of observed space charge fields[25] but also because of high current signals in most polymers tested.[1]

The present work has shown that at low temperatures the last problem should be given a detailed consideration as an effect of electron charging suddenly went to the forefront. We start this work with a careful examination of our traditional setup in its basic configuration (Fig. 6). Actually, it is a famous scheme proposed by Gross in early 1970s and known as the split Faraday cup technique.[26,27]

Gross's experiments refer to charging a sample with no applied voltage studying the basic laws of the charging process while our main interest lies in the polymer RIC characterization. In position a of the switch, we measure a current I_2 from a rear electrode *4* using it as a zero voltage signal (the so-called radiation-driven
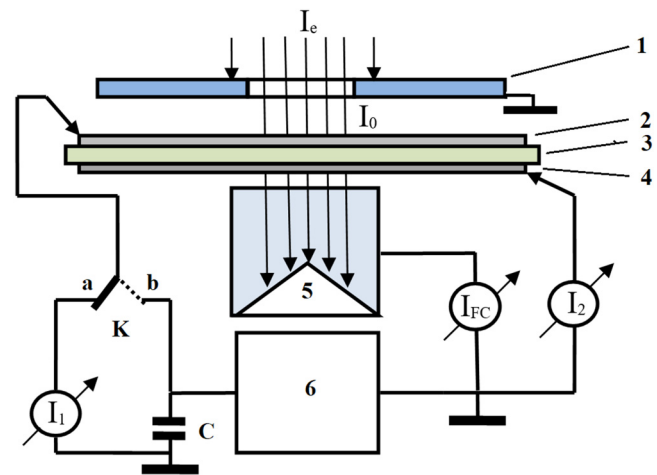
FIG. 6. Schematic representation of the measuring setup. 1—collimator; 2—potential electrode; 3—test sample; 4—measuring electrode; 5—Faraday cup; 6—voltage source. C is a capacitor used to suppress the rf-noise in the circuit in an operating mode; K is a two-position switch (in position a shown in the picture, both electrodes 2 and 4 are grounded, in position b, potential electrode 2 is under applied voltage).

current) to be subtracted from I_2 measured with an applied voltage V_0 (switch in position b). This signal when reduced to the conductivity γ is taken to mean the RIC γ_r of a polymer (see Ref. 8 for details).

Room-temperature measurements encountered no problems and a current limitation at t_m for a step-function irradiations was uniquely ascribed to the bimolecular recombination of the Langevin type used in the RFV model.[1] At 103 K, we encountered a slight instability of a zero-voltage signal I_2. In addition, large space charge fields were expected to appear during long-time irradiations starting from the current maximum at t_m. For their estimation, we used the theory of an electron deposition by beams of high energy electrons developed by Evdokimov and Gusel'nikov in Tomsk Polytechnique (Russia)[28] and further elaborated in Refs. 29–32.

It is assumed that both the dose rate R_0 and the electron deposition rate $q_0 = -eS_0$ (q_0 in A/m^3 and S_0 in m^{-3} c^{-1}) are uniform and constant and the RIC of a polymer may be described by the RFV model [Eq. (6)]. Zero initial conditions are used. Coordinate x is directed from a front electrode ($x = 0$) to a rear one ($x = L$). The boundary condition is as follows:

$$\int_0^L F_c(x, t)dx = 0, \qquad (8)$$

where $F_c(x, t)$ is an electric field inside a sample.

This theory is better discussed using a schematic representation of our measuring circuit duplicating Gross's split Faraday cup technique (Fig. 6).[26]

In the operating mode (switch position b), an irradiated polymer sample is subjected to two electric fields acting simultaneously: one due to an applied constant voltage $V_0 = F_0 L$ (L is the sample thickness) and F_e is the space charge field (time and coordinate dependent) emerging as a result of an intricate interaction of excess electrons (clear minority) and an ambient electron-hole majority. First are responsible for an electron charging and the second accounts for the RIC. Each beam electron stopping in a sample produces about 1500 geminate pairs (see Sec. IV). Thus, a concentration of excess electrons is by far less than a total concentration of the generated geminate pairs. Both fields produce currents, which originate from the same RIC defined by the RFV equations. Now, we follow an exact analytical solution found in Ref. 30.

The above-mentioned theory predicts that the space charge field F_e is a linear function of coordinate x directed inside a polymer film,

$$F_c(x, t) = \frac{e}{\varepsilon \varepsilon_0} \times (L/2 - x) \times \frac{S_0}{g_0} N(t), \qquad (9)$$

where $N(t)$ is the total concentration of electrons, which is given by Eq. (6). Note it is not coordinate dependent unlike a space charge field F_e which is equal to zero at the middle of a sample ($x = L/2$) where this field reverses sign. The maximum fields (by module) occur at electrodes ($x = 0$ or L) and in the steady-state condition

are equal to

$$F_{\max} = \frac{1}{2} \times \frac{eS_0 L}{\tilde{\gamma}_r}. \qquad (10)$$

In experimental scheme (Fig. 6), the total injection (electron deposition) current $I_0 = I_1 + I_2 = -eS_0L$ divides into two electrode currents each equal to $I_0/2$ so that Eq. (10) takes the form

$$F_{\max} = \frac{I_0}{2\tilde{\gamma}_r}. \qquad (11)$$

In reality, the electron charging is not uniform as currents I_1 and I_1 may not be equal so the above equation should be applied separately for each electrode this time without a factor ½ (I_0 should be replaced with respective I_1 or I_2). One should remember that these estimations refer to the steady-state condition only.

To clarify the situation, we repeated the long-time irradiations with PET-2 samples. Experimental results concerning K_{rm} and t_m are given in Table I and Fig. 3. In the last case (below, we use arithmetic values), I_0 constituted 20% of the beam current density so that for $I_b = 3.5$ nA/cm^2, $I_0 = 0.7$ nA/cm^2 with $I_2 = 0.46$ nA/cm^2 and $I_1 = 0.24$ nA/cm^2.

We see that currents are not equal indeed but we continue to use the above theory to get insight into the charging process. So, we use averaged values of these currents $I_1 = I_2 = 0.35$ nA/cm^2. Now, we determine the ratio $S_0/g_0 = 1.5 \times 10^{-3}$ for $R_0 = 22$ Gy/s corresponding to $I_b = 3.5$ nA/cm^2. Numerical results are represented in Fig. 7.
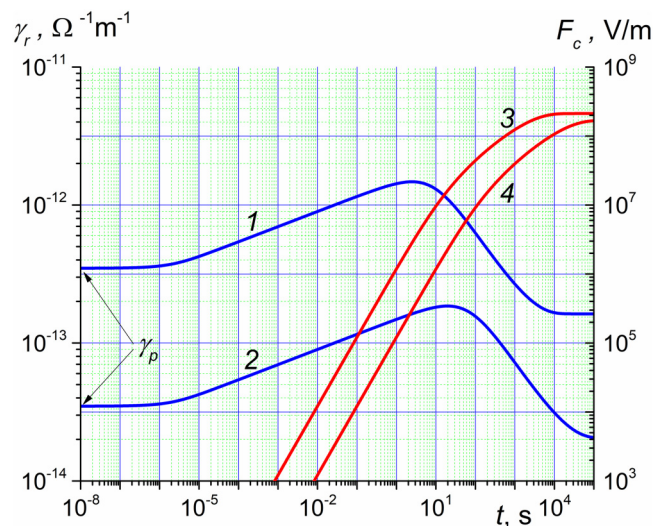

FIG. 7. Numerical calculations for PET-2 sample for an electron beam current density 3.5 (curves *2, 4*) and 35 nA/cm^2 (curves *1, 3*) and a dose rate 22 (curves *2, 4*) and 220 Gy/s (curves *1, 3*). Curves *1* and *2* refer to the RIC while curves *3* and *4* refer to a space charge field at the front electrode. Arrows indicate the values of the prompt RIC for curves *1* and *2*.

We see that F_e at $t_m = 40$ s (curve *2*) is about 6×10^6 V/m (curve *4*) and even at ten times longer time it still stays only reasonably high (2.5×10^7 V/m). But at equilibrium, it reaches 2×10^8 V/m making an interpretation of experimental results totally confusing. Not so at t_m when the total field changes from 4.6×10^7 at $x = 0$ to 3.4×10^7 V/m at $x = L$, the mean value being F_c. In our case, the volt-ampere characteristic of the RIC is expected to be mild and the traditional data reduction of current transients is quite appropriate. Curves *3* and *4* approach each other in the limit $t \to \infty$ but not coincide: curve *3* is still slightly higher. Indeed, I_0 is proportional to I_b while $\tilde{\gamma}_r \propto R_0^\Delta \propto I_b^{0.89}$ in PET-2 so that according to Eq. (11), we have $F_{max} \propto I_b^{0.11}$ and it slightly rises with the beam current density.

Calculated curves *2* and *4* allow assessing of the contributions of the displacement current density $j_d(t) = \varepsilon\varepsilon_0 \partial F_c(0, t)/\partial t$ and the conduction current density $j_c(0, t) = \gamma_r(t) F_c(0, t)$ at the left electrode. For $t \ll t_m$, the first term grossly dominates. Even at t_m, it is almost three times larger. Only at times longer than 10^5 s, the above ratio is reversed.

It is tempting to use Eq. (11) in which $\tilde{\gamma}_r$ is replaced with γ_{rm}. Figure 7 shows that such an operation is erroneous as it is overestimating the current value of F_e by four times while underestimating F_{max} by five times. The Maxwell relaxation time is as follows:

$$t_{rel} = \varepsilon\varepsilon_0/\tilde{\gamma}_r, \quad (12)$$

where ε is taken to be equal to 3.2 in our polymers. For $\gamma_{rm} = 1.3 \times 10^{-13}$ Ω^{-1} m^{-1}, it is approximately equal to 22 s. This time is comparable to an experimental $t_m = 25$ s in PET-2 at a dose rate of 22 Gy/s but as we have shown this near coincidence fails to
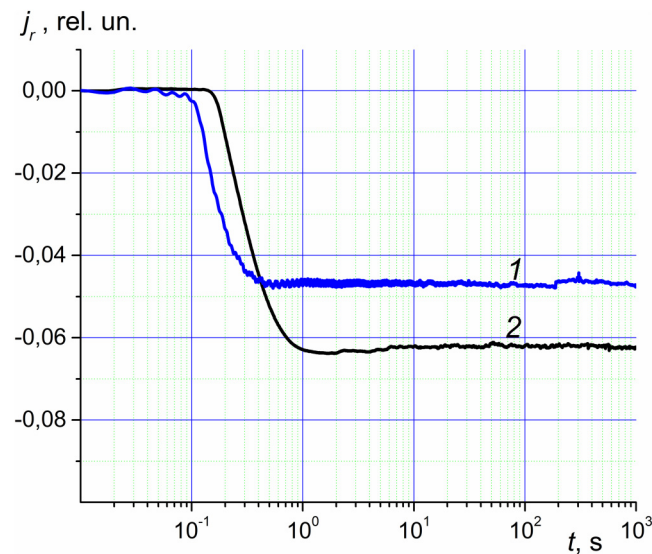
secure an application of Eq. (11) with the above-mentioned substitution.

The main problem of RIC measurements is a potential time dependence of current $I_2(t)$ which, as we already know, serves as the reference line in estimating a voltage-produced change in this current. The simplest case implies that $I_2 = $ constant as the theory of Refs. 29–32 has it. In reality, a dose rate and an electron deposition rate are not uniform across a sample and we have to wait an equilibration time of the MT processes given by the RFV model (and not simply t_{rel}) to reach a real equilibrium. We made a number of experiments to clarify $I_2(t)$ dependence during step-function irradiations (Fig. 8). It is seen that in a carefully conducted experiment $I_2(t)$ is constant to within 10% if a beam current I_b has a box-like form.

Assuming that the current $I_2(t)$ is the same for both positions of the switch K (*a* and *b* in Fig. 6), we may use it for estimating $\gamma_r(t)$ as in Ref. 8. Situation with Kapton is more severe. Due to increased thickness, the ratio I_0/I_b increases to 0.54 but now the role of electrodes interchange and $F_{max} \approx 4 \times 10^7$ V/m at the front electrode (here F_e is always positive). The total field at $x = 0$ becomes 8×10^7 V/m at t_m (rough estimates for $R_0 = 250$ Gy/s) while at $x = L$ it reduces to 1.5×10^7 V/m (now, F_{max} becomes negative and equal approximately to minus 2.5×10^7 V/m).

Thus, an electric field changes considerably (in Kapton, by five times) inside a sample. But as long as K_{rm} is field independent, the RIC kinetics $\gamma_r(t)$ is reproduced authentically by the measured current density $j_r(t)$. This property is due to a multiplicative form of Eq. (9), which contains factors with separated variables. But this happens because we are interested in the temporal form of the RIC current only. But this factor degrades appreciably an accuracy of the current–voltage characteristics taken during long-time irradiations in the first place. Experiments using electron guns with an increased electron energy or even x-ray tubes are clearly preferable.

VI. DISCUSSION

As it has been already said in Sec. IV, we continue to use the RFV model for RIC description at low temperatures repeating argumentation given earlier in Ref. 3. But two important ideas have been taken into consideration. First, about the generation of geminate electrons as *free* electrons drifting along field lines formed by the combination of an applied electric field and of the Coulomb field of a sibling hole (diffusion neglected). In this situation, a geminate recombination process becomes highly protracted with time t_{inv} given by Eq. (7). Second, despite the fact that diffusion is neglected, the MT transport involves a fast electron displacement $\mu_0\tau_0(F_0 + F_c)$ after each detrapping act, which is especially effective at early transport times.

But, when we are trying to estimate an average recombination time at a small electric field [see Eq. (6) in Ref. 3], the result is unacceptably high. Here, one has to accept an idea of an electron drifting through an ensemble of deep isoenergetic traps as proposed by Yakovlev *et al.*,[4,5] which is effectively a one-trap RFV model. Their approach predicts geminate recombination times in frozen hydrocarbon liquids at 77 K around 1000 s, which are close to the experimental results.[4]

j_r, rel. un.

FIG. 8. Experimental $I_2(t)$ curves observed in PET-2 (curve *1*) and Kapton (curve *2*) at $I_b = 9.6$ nA/cm^2 ($R_0 = 60$ or 75 Gy/s, respectively). Shutter gets fully open at 0.3 s after having been activated. The maximum RIC current in both polymers at 4×10^7 V/m exceeds I_2 by up to 2.5 times.

RIC measurements in polymers using 50 keV electrons are inseparably linked with the formation of a space charge field due to beam electrons stopping in a sample. Such an electron produces about 1500 geminate pairs (see Sec. IV). Thus, a concentration of excess electrons responsible for the charging effect is by far less than the total concentration of generated geminate pairs. An irradiated polymer sample is subjected to two electric fields acting simultaneously: one due to an applied constant voltage $V_0 = F_0 L$ (L is the sample thickness) and F_e is the space charge field (time and coordinate dependent) emerging as a result of an intricate interaction of excess electrons (clear minority) and an ambient electron-hole majority. First are responsible for an electron charging and the second accounts for the RIC. This line of reasoning assumes implicitly that these phenomena may be considered separately, which is a common practice now and we have followed it so far. Nevertheless, this question deserves more detailed consideration in future.

We have already seen that the most stable RIC results relating to the main characteristics of long-time irradiations at 103 K such as t_m and Δ [see Eq. (3)] belong to PET-2 samples. Indeed, curve _1_ in Fig. 3 unlike all others except theoretical curve _5_ exhibits a regular behavior slightly milder than $t_m \propto R_0^{-1}$, which is compatible with the RFV prediction following from Eq. (3). Also, data from Fig. 7 confirm this assertion. Our results testify certainly in favor of the validity of the RFV model even at low temperatures. To ease electron charging effects in test samples observed for 50 keV electron beams used in the present study, one is recommended, when possible, to employ x-ray tubes as in Ref. 33.

VII. CONCLUSIONS

Pulsed and long-time (continuous) irradiations of PET and Kapton at 103 K have shown that the long-time RIC generally exceeds the prompt conductivity by several times only and could be easily evaluated [see Eq. (2)] using reduced conductivity K_{rm} (see Fig. 4). This estimation solves all engineering problems about RIC of spacecraft polymers at the lowest temperatures encountered on outer satellite surfaces and allows assessing an increasing risk of surface electrostatic discharges on board an operating spacecraft.

From a scientific point of view, our results show that the MT formalism employed in the RFV model describes the charge carrier transport in tested polymers even at temperatures as low as 103 K if the due account of the earlier work by Arkhipov _et al._[7] and to a less extent of the results of Yakovlev _et al._[4,5] has been made. We failed to establish the exact nature of the time t_m (10–100 s) when the RIC current under continuous irradiation reaches a maximum. After this time, a recombination-limited regime sets in but its description is still lacking. Although t_m is rather close to predictions of the RFV model[2] and to Arkhipov _et al._[6,7] analytical results, some discrepancies between theory and experiment have been noted and discussed in detail.

There is a need of fulfilling computer simulations of a geminate RIC conductivity in disordered solids similar to what has been done in Ref. 24 where numerical calculations have been fulfilled for an ideal trap-free dielectric.

To promote further scientific exploration of the RIC (current–voltage characteristics, recombination process, dose effects), one

should take additional measures to reduce the space charge field arising from beam electrons being stopped in a test sample, an effect especially prominent at low temperatures, for example, by using MeV electron accelerators or x-ray tubes. Also, using as thin samples as possible is imperative.

At last, we believe that in near future composite polymers generally[34,35] and those with enhanced electrical conductivity, in particular, securing an efficient charge drain to the spacecraft frame and thus eliminating on-board electrostatic discharges[36–38] will find a wide application in the spacecraft industry. So, we are planning to investigate the RIC in such materials at low temperatures.

AUTHOR DECLARATIONS
Conflict of Interest

The authors have no conflicts to disclose.

Author Contributions

Andrey Tyutnev: Conceptualization (equal); Investigation (equal); Supervision (equal). **Vladimir Saenko:** Investigation (equal); Methodology (equal). **Ilshat Mullakhmetov:** Investigation (equal); Methodology (equal); Software (equal). **Evgenii Pozhidaev:** Conceptualization (equal); Resources (equal); Supervision (equal).

DATA AVAILABILITY

The data that support the findings of this study are available from the corresponding author upon reasonable request.

REFERENCES

[1]A. Tyutnev, V. Saenko, E. Pozhidaev, and R. Sh Ikhsanov, IEEE Trans. Plasma Sci. **43**, 2915 (2015).
[2]A. P. Tyutnev, V. S. Saenko, R. Sh. Ikhsanov, and E. Krouk, J. Appl. Phys. **126**, 095501 (2019).
[3]A. Tyutnev, V. Saenko, I. Mullakhmetov, and A. Abrameshin, J. Appl. Phys. **132**, 135105 (2022).
[4]B. S. Yakovlev, K. K. Ametov, and G. F. Novikov, Radiat. Phys. Chem. **11**, 219 (1978).
[5]B. S. Yakovlev and L. V. Lukin, Adv. Chem. Phys. **60**, 99 (1985).
[6]V. I. Arkhipov, Phiz. Techn. Poluprov. **20**, 556 (1986) (in Russian or see Ref. 2 in Ref. 7).
[7]V. I. Arkhipov, V. R. Nikitenko, and A. I. Rudenko, Sov. Phys. Semicond. **21**, 685 (1987).
[8]A. Tyutnev, V. Saenko, A. Zhadov, and E. Pozhidaev, Polymers **11**, 2061 (2019).
[9]A. Tyutnev, V. Saenko, A. Zhadov, and E. Pozhidaev, IEEE Trans. Plasma Sci. **47**, 3739 (2019).
[10]A. Tyutnev, R. Ihksanov, V. Saenko, and V. Ashmarin, J. Appl. Phys. **128**, 225501 (2020).
[11]L. Onsager, Phys. Rev. **54**, 554 (1938); A. Hummel, Adv. Rad. Chem. **4**, 1 (1974).
[12]K. M. Hong and J. Noolandi, J. Chem. Phys. **68**, 5163 (1978).
[13]G. R. Freeman, _Kinetics of Non-Homogeneous Processes_ (Wiley, New York, 1987).

08 September 2023 05:38:44

[14] A. Tyutnev, V. Saenko, and E. Pozhidaev, IEEE Trans. Plasma Sci. **46**, 645 (2018).

[15] V. R. Nikitenko, A. P. Tyutnev, V. S. Saenko, and E. D. Pozhidaev, Khim. Fiz. **23**, 92 (2004) (in Russian).

[16] R. C. Hughes, IEEE Trans. Nucl. Sci. **18**, 281 (1971).

[17] A. Hummel and W. F. Schmidt, Rad. Res. Rev. **5**, 199 (1974).

[18] A. P. Tyutnev, V. S. Saenko, R. Sh. Ikhsanov, V. N. Abramov, and E. D. Pozhidaev, High Energy Chem. **42**, 29 (2008).

[19] R. C. Hughes, in *Proceedings of 2nd International Conference on Electrophotography, Washington DC, USA, 24–27 October*, edited by D. R. White (Society of Photographic Scientists and Engineers, 1975), pp. 147–151.

[20] V. I. Arlkhipov, A. P. Tyutnev, and V. R. Nikitenko, Chem. Phys. Rep. **15**, 419 (1996).

[21] V. R. Nikitenko, A. P. Tyutnev, V. S. Saenko, and E. D. Pozhidaev, Khim. Fiz. **25**, 61 (2006) (in Russian).

[22] A. P. Tyutnev, V. N. Abramov, V. S. Saenko, E. D. Pozhidaev, and A. A. Floridov, Khim. Fiz. **13**, 109 (1994) (in Russian).

[23] S. R. Kurtz and R. C. Hughes, J. Appl. Phys. **54**, 229 (1983).

[24] R. Sh. Ikhsanov, A. P. Tyutnev, V. S. Saenko, and E. D. Pozhidaev, Russ. J. Phys. Chem. B **2**, 309 (2008).

[25] A. P. Tyutnev, D. N. Sadovnichii, V. S. Saenko, and E. D. Pozhidaev, Polym. Sci. A **47**, 1174 (2005).

[26] B. Gross, G. M. Sessler, and J. E. West, J. Appl. Phys. **45**, 2841 (1974).

[27] B. Gross, "Radiation induced charge storage and polarization," in *Electrets*, edited by G. M. Sessler (Springer-Verlag, New York, 1980).

[28] O. B. Evdokimov and V. N. Gusel'nikov, Khim. Vysok. Energy **8**, 423 (1974) (in Russian).

[29] A. P. Tyutnev *et al.*, *Electrical Processes in Polymers Under Irradiation* (Energoatomizdat, Moscow, 1985) (in Russian).

[30] A. P. Tyutnev *et al.*, *Radiation Electrophysics in Organic Dielectrics* (Energoatomizdat, Moscow, 1989) (in Russian).

[31] V. I. Arkhipov and I. A. Perova, J. Phys. D: Appl. Phys. **26**, 1301 (1993).

[32] A. P. Tyutnev, Y. F. Kundina, V. S. Saenko, A. N. Doronin, and E. D. Pozhidaev, High Perform. Polym. **13**, S493 (2001).

[33] B. Gross, R. M. Faria, and G. F. Leal Ferreira, J. Appl. Phys. **52**, 571 (1981).

[34] T. K. Das, P. G. Das, and N. C. Das, Adv. Compos. Hybrid Mater. **2**, 214 (2019).

[35] M. Goyal, S. N. Agarwal, and N. Bhatnagal, J. Appl. Polym. Sci. **139**, e52816 (2022).

[36] V. S. Saenko, A. P. Tyutnev, M. A. Afanasyeva, and A. E. Abrameshin, IEEE Trans. Plasma Sci. **47**, 3648 (2019).

[37] V. Saenko, A. Tyutnev, A. Abrameshin, and G. Belik, IEEE Trans. Plasma Sci. **45**, 1843 (2017).

[38] D. A. Abrameshin, E. D. Pozhidaev, V. S. Saenko, and S. R. Tumkovskiy, IEEE Trans. Plasma Sci. **47**, 3653 (2019).